Research Article

Cancer Prevention Research

Combination Effects of Salvianolic Acid B with Low-Dose Celecoxib on Inhibition of Head and Neck Squamous Cell Carcinoma Growth *In vitro* and *In vivo*

Yuan Zhao[1,4], Yubin Hao[1,6], Hongguang Ji[7], Yayin Fang[2], Yinhan Guo[5], Wei Sha[1,4], Yanfei Zhou[1], Xiaowu Pang[1], William M. Southerland[2], Joseph A. Califano[6], and Xinbin Gu[1,3]

Abstract

Head and neck squamous cell carcinoma (HNSCC) development is closely associated with inflammation. Cyclooxygenase-2 (COX-2) is an important mediator of inflammation. Therefore, celecoxib, a selective inhibitor of COX-2, was hailed as a promising chemopreventive agent for HNSCC. Dose-dependent cardiac toxicity limits long-term use of celecoxib, but it seems likely that this may be diminished by lowering its dose. We found that salvianolic acid B (Sal-B), isolated from *Salvia miltiorrhiza* Bge, can effectively suppress COX-2 expression and induce apoptosis in a variety of cancer cell lines. In this study, we report that combination of Sal-B with low-dose celecoxib results in a more pronounced anticancer effect in HNSCC than either agent alone. The combination effects were assessed in four HNSCC cell lines (JHU-06, JHU-011, JHU-013, and JHU-022) by evaluating cell viability, proliferation, and tumor xenograft growth. Cell viability and proliferation were significantly inhibited by both the combined and single-agent treatments. However, the combination treatment significantly enhanced anticancer efficacy in JHU-013 and JHU-022 cell lines compared with the single treatment regimens. A half-dose of daily Sal-B (40 mg/kg/d) and celecoxib (2.5 mg/kg/d) significantly inhibited JHU-013 xenograft growth relative to mice treated with a full dose of Sal-B or celecoxib alone. The combination was associated with profound inhibition of COX-2 and enhanced induction of apoptosis. Taken together, these results strongly suggest that combination of Sal-B, a multifunctional anticancer agent, with low-dose celecoxib holds potential as a new preventive strategy in targeting inflammatory-associated tumor development. *Cancer Prev Res; 3(6); 787–96. ©2010 AACR.*

Introduction

Head and neck squamous cell carcinoma (HNSCC) represents >90% of all head and neck cancers (1). Although tobacco exposure is the primary etiologic environmental agent associated with HNSCC, development of this tumor is associated with pathways that are also active in the inflammatory response (2). Chronic inflammatory microenvironment gradually leads to cellular proliferation and multiple genetic alterations, inducing early malignant changes from normal epithelial cell to cancer cell (3). Thus, it remains an appealing strategy to develop effective, nontoxic, and affordable novel pharmacologic agents for preventing development of both HNSCC and second primary HNSCC (4–6).

Celecoxib is a nonsteroidal anti-inflammatory drug (NSAID) that helps to control inflammation by inhibiting cyclooxygenase-2 (COX-2) activity (7). Celecoxib was hailed as a promising cancer prevention drug and has been tested in several clinical studies (8–11). However, it was found to be associated with a dose-dependent cardiovascular morbidity, which limited its long-term use as a cancer prevention agent (7, 12–14).

Salvianolic acid B (Sal-B) is a leading bioactive component of *Salvia miltiorrhiza* Bge (Danshen or Tanshen) and used as a quality control ingredient and active marker for *S. miltiorrhiza* Bge products by the National Pharmacopoeia Council of China. *S. miltiorrhiza* Bge is a well-known Chinese herbal medicine that has been used for thousands of years to treat cardiovascular diseases, chronic hepatitis, liver fibrosis, and tumoral diseases without undesirable side effects (5, 15–19). Based on the theory of traditional Chinese medicine, *S. miltiorrhiza* Bge has its effect by promoting blood circulation to repair damaged tissues. Additionally, *S. miltiorrhiza* Bge and Sal-B have been shown to inhibit inflammation (5, 19, 20), coagulation

Authors' Affiliations: Departments of [1]Oral Diagnostic Service and [2]Biochemistry and Molecular Biology and [3]Cancer Center, Howard University, Washington, District of Columbia; [4]Beijing University of Chinese Medicine; [5]Oriental TenGen Tech Development Co. Ltd., Beijing, China; [6]Department of Otolaryngology-Head and Neck Surgery, The Johns Hopkins University, Baltimore, Maryland; and [7]Shanghai TenGen Biomedical Co. Ltd., Shanghai, China

Corresponding Author: Xinbin Gu, Department of Oral Diagnostic Service, Howard University College of Dentistry, 600 West Street, NW, Washington, DC 20059. Phone: 202-806-0345/202-907-8454; Fax: 202-806-0446; E-mail: xgu@howard.edu.

doi: 10.1158/1940-6207.CAPR-09-0243

(21), oxidation (22), and tumor growth (5, 23–25). Our previous study found that Sal-B widely suppresses proliferation of human cancer cell lines, including HNSCC, prostate, breast, and liver cancers (5). These anticancer activities are through not only selectively inhibiting COX-2 mRNA expression but also effectively inducing apoptosis in cancer cells (5). However, there was a report indicating that Sal-B plays as an antioxidant to modulate hydrogen peroxide–induced apoptosis through the phosphoinositide 3-kinase–Akt–Raf–mitogen-activated protein/extracellular signal-regulated kinase kinase–extracellular signal-regulated kinase pathway (26). As a promising natural anticancer agent, more studies are needed to understand the anticancer mechanism and clinical application.

In recent years, combination treatment has received increased attention (27–29) because it has the potential to enhance the therapeutic effect and reduce toxicity by lowering the dose required for each agent (30). In this study, we tested the hypothesis that combination of Sal-B and low-dose celecoxib may result in a more pronounced anticancer effect in HNSCC cell growth when compared with either agent alone using *in vitro* and *in vivo* studies.

Materials and Methods

Chemical reagents

Sal-B was isolated from *S. miltiorrhiza* Bge as previously described (5). Celecoxib was extracted from commercially available 200 mg Celebrex capsules with ethyl acetate aqueous solution (5).

Cell lines and culture

HNSCC cell lines (JHU-06, JHU-011, JHU-013, and JHU-022) were obtained from The Johns Hopkins University. The HNSCC cells were grown in RPMI 1640. The cultures were supplemented with 10% fetal bovine serum and an antibiotic-antimycotic mixture (100 IU/mL penicillin and 100 μg/mL streptomycin; Cellgro). All cells were grown in 5% CO_2 at 37°C and subcultured at an initial density of 1×10^5/mL every 3 to 4 days. All experiments were done with cells in the logarithmic phase of growth.

MTT assay

Cells (10,000 per well density) were seeded in flat-bottomed 96-well cell culture plates in a proper medium with 2% fetal bovine serum. The cells were then treated with 100 μmol/L Sal-B and 10 μmol/L celecoxib individually and with 50 μmol/L Sal-B plus 5 μmol/L celecoxib in combination for 24 hours. Twenty microliters of MTT (5 mg/mL) solution (Sigma) were added to each well at 37°C for 4 hours. After removing the media, 200 μL of DMSO were added and left for 30 minutes at room temperature to dissolve the formazan crystals in shaker. The absorbance at 560 nm was measured in a microplate reader (Bio-Rad).

Flow cytometry

To analyze cell cycle, JHU-022 cells were cultured without serum for 24 hours and then treated with Sal-B (100 μmol/L), celecoxib (10 μmol/L), or a half-dose of combination for 24 or 48 hours. The treated cells were collected, washed, and fixed in chilled 80% ethanol. The fixed cells were washed twice in PBS and then incubated with a solution containing 100 μg/mL RNase at 37°C water bath for 30 to 45 minutes. Twenty-five to 50 μL of propidium iodide (final concentration, 50 μg/mL) were added to the cells, which were incubated at 37°C water bath for 15 minutes. The cell cycle was analyzed by flow cytometry. Ten thousand cells per sample were analyzed for both assays. To analyze levels of COX-2 protein, the treated HNSCC cells were collected, washed, and fixed in chilled 80% ethanol. The fixed cells were washed twice in PBS and then incubated with a solution containing COX-2–FITC (1:200; Chemical Co.) in the dark for 30 minutes at room temperature. The COX-2 level was determined by FACStar flow cytometry (Becton Dickinson & Co.).

Human tumor xenografts in athymic (nude) mice

Four-week-old male athymic nude mice (*nu/nu*) were obtained from Harlan Sprague Dawley, Inc. They were provided Harlan Teklad #2018 Global 18% Protein Rodent Diet and water *ad libitum*. Mice were housed in temperature-controlled rooms (74 ± 2°F) with a 12-hour alternating light-dark cycle. JHU-013 cells (2×10^6/100 μL/mouse) were injected s.c. into the lower backs of the mice using a 25-gauge needle in left and right sides. All animals were then randomly assigned to four groups (five mice per group) with topical treatment for 24 days following JHU-013 cell inoculation: Sal-B–treated (80 mg/kg/d), celecoxib-treated (5 mg/kg/d), combination-treated (40 mg/kg/d Sal-B and 2.5 mg/kg/d celecoxib), and untreated control group by i.p. administration every day. Body weights were measured once a week. Autopsy in these animals revealed tumor masses, and tumor size and weight were measured. Guidelines for the humane treatment of animals were followed as approved by the Howard University Animal Care and Use Committee.

Histologic evaluation of tumor burden

Paraffin-embedded JHU-013 cancer cell tissue sections were used for the histologic determination of tumor structure. Tissue sections from each group of rats were stained with H&E (American HistoLabs, Inc.).

Immunohistochemical staining

Paraffin-embedded nude mouse xenograft tissue was done using LSAB2 System-HRP kit following the standard manufacturer's protocol (DakoCytomation). Paraffin-embedded tumor specimens were deparaffinized in xylene and rehydrated in graded alcohol. Endogenous peroxidase was blocked using hydrogen peroxide for 20 minutes. The slides were incubated with primary antibody of proliferating cell nuclear antigen (PCNA; 1:100; EMD) overnight at 4°C and then incubated with second antibody for 2 hours at room temperature. Binding streptavidin–horseradish

peroxidase (HRP) was 20 minutes at room temperature. Staining time of 3,3′-diaminobenzidine solution depended on the sample condition. The stained slides were visualized on a microscope. Images were captured with an attached camera linked to a computer. For quantitative analysis of immunohistochemistry and H&E staining, 10 fields were randomly selected for each slide from three different mice. We manually counted the number of positive cell and total number of cells. The percentage of positive cells of the total number of cells was calculated for each image.

Quantitative real-time PCR

RNA was extracted from the treated cells based on the RNeasy Mini kit protocol (Qiagen). First-strand cDNA was synthesized by PCR using a SuperScript III system with oligo(dT) primers (Invitrogen). The expression levels of COX-2 were measured by real-time reverse transcription-PCR using Taqman Universal PCR Master Mix (Applied Biosystems) with COX-2 primer (6-FAM–labeled probe, Hs00153133_m1). A β-actin (4333762T) primer was used as an endogenous control. The real-time PCR was done in triplicate for each gene. AmpliTaq Gold Enzyme was first activated at 95°C for 10 minutes followed by 40 cycles, including denaturation at 95°C for 15 seconds and annealing at 60°C for 1 minute. The data were analyzed using MxPro-Mx3000p software and analyzed using $2^{-\Delta\Delta CT}$ method (31).

Prostaglandin E_2 level

Prostaglandin E_2 (PGE_2) levels were evaluated as an indication of level of COX-2 activity. JHU-013 cells were treated with Sal-B (100 μmol/L), celecoxib (10 μmol/L), and combination (50 μmol/L Sal-B plus 5 μmol/L celecoxib) in RPMI 1640 with 2% fetal bovine serum. The culture medium was collected, and the level of PGE_2 was determined by a Correlate-EIA Prostaglandin E_2 Enzyme Immunoassay kit (Assay Designs) at absorbances (Bio-Rad) of 405 and 570 nm. The PGE_2 level was calculated as a unit of pg/mL as per instructions provided by the manufacturer of the assay kit.

Terminal deoxynucleotidyl transferase–mediated dUTP nick end labeling assay

Apoptotic cell death in deparaffinized tissue sections (American HistoLabs) was determined by terminal deoxynucleotidyl transferase (TdT)–mediated dUTP nick end labeling (TUNEL) technique using TdT-FragEL DNA Fragmentation Detection kit (EMD). This method is based on the specific binding of TdT to 3′-OH end of DNA and ensuring synthesis of polydeoxynucleotide polymer. Briefly, deparaffinized sections were digested using proteinase K, and endogenous peroxidase activity was blocked using 3% hydrogen peroxide in 10 mmol/L Tris (pH 8.0). The sections were then placed in equilibration buffer and incubated with TdT enzyme in a humid chamber at 37°C for 1.5 hours. The reaction was terminated with stop buffer and incubated with HRP for 30 minutes. The apoptotic nuclei were stained by 3,3′-diaminobenzidine and observed under microscope. Ten fields were randomly selected for each slide. Each field was then photographed at a magnification of ×20. We manually counted the numbers of positively stained nuclei for TUNEL. The percentage of positive cells of the total number of cells was calculated for each image.

Western immunoblotting

Whole-cell lysates were prepared from treated JHU-013 and JHU-022 cells incubated with radioimmunoprecipitation assay lysis buffer kit (Santa Cruz Biotechnology), and protein concentrations were quantified using a Bio-Rad protein assay. Whole-cell proteins (30 μg) were separated by 8% SDS-PAGE gel, transferred to a polyvinylidene difluoride membrane (Amersham Corp.), and then probed sequentially with antibodies against the following proteins: COX-2, epidermal growth factor receptor (EGFR), p53, Bcl-2, and β-actin (Sigma). Washed blots were then incubated with HRP-conjugated anti-rabbit, anti-mouse, or anti-goat antibody (Santa Cruz Biotechnology) for 1 hour at room temperature. Blots were developed by a peroxidase reaction using the enhanced chemiluminescence detection system (Bio-Rad).

Statistical analyses

Results were presented relative to untreated controls. Values represent the mean ± SD of a minimum of three replicate tests. Data were analyzed by the Duncan test following the ANOVA procedure when multiple comparisons were made. Differences were considered significant when $P < 0.05$.

Results

Effect of Sal-B in combination with celecoxib on inhibition of HNSCC growth *in vitro*

Four HNSCC cell lines (JHU-06, JHU-011, JHU-013, and JHU-022) were used for testing the effectiveness of the combined therapeutic regimen (Fig. 1A). The cells were first treated with Sal-B (100 μmol/L) alone and celecoxib (10 μmol/L) alone or a half-dose of Sal-B (50 μmol/L) and celecoxib (5 μmol/L) combination for 24 hours. After treatment, cell viability was measured using the MTT assay. Overall, both the individual agent and the combination treatments elicited decreased cell viability and proliferation in all four HNSCC cell lines. There was a significant reduction of cell viability in JHU-013 and JHU-022 cell lines with the combination treatment relative to the individual agent treatments (Fig. 1A).

Effect of Sal-B in combination with celecoxib on cell cycle in HNSCC

Cell cycle activity was analyzed after JHU-022 cells were treated with Sal-B (100 μmol/L) alone, celecoxib (10 μmol/L) alone, or Sal-B (50 μmol/L) with celecoxib (5 μmol/L) in combination for 24 and 48 hours, respectively (Fig. 1B; Table 1). Again, all treatments resulted in increased G_0-G_1 phase and decreased G_2-M and S phases of

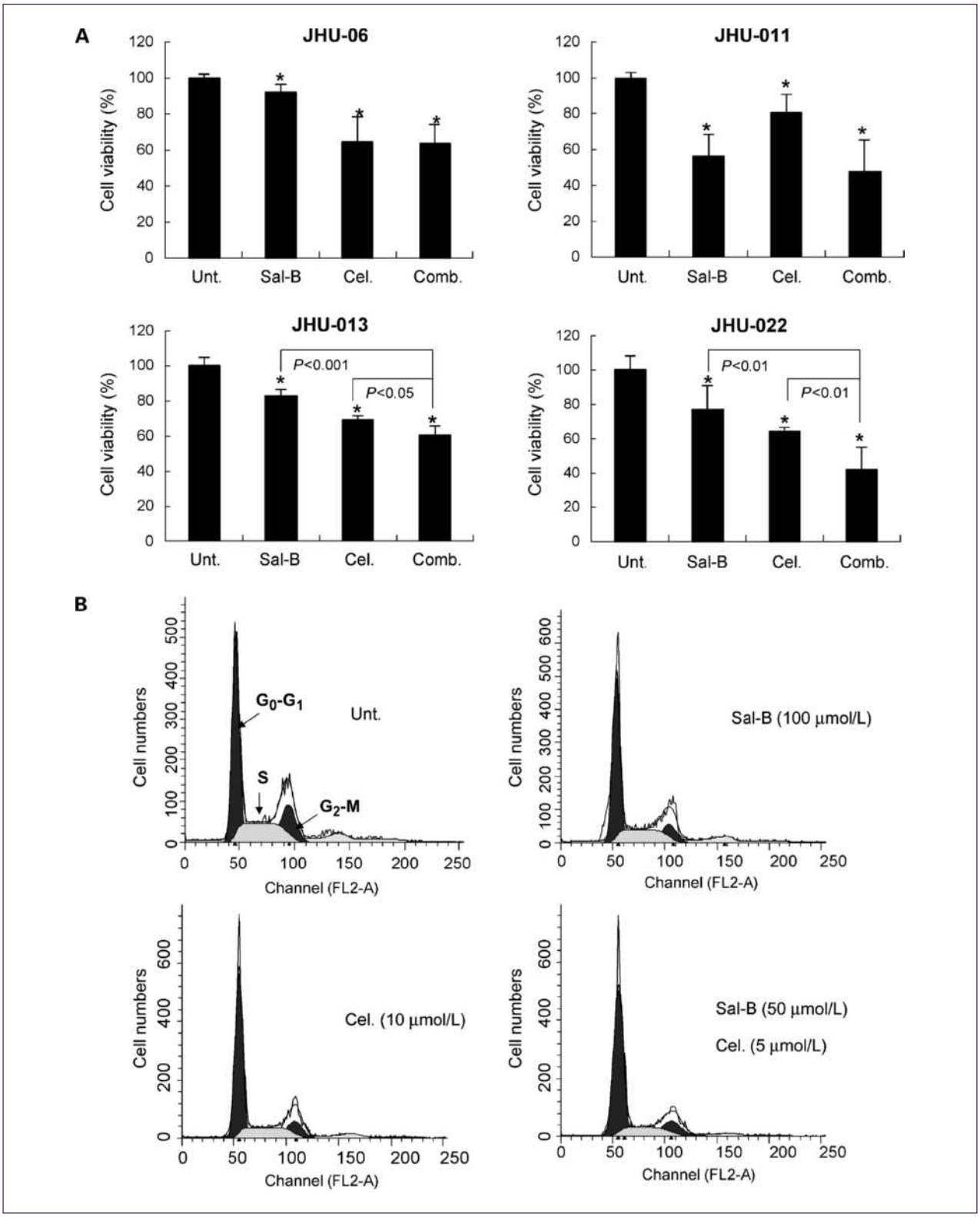

Fig. 1. Effect of Sal-B and celecoxib, alone and in combination, on the inhibition of HNSCC cell proliferation *in vitro*. A, four HNSCC cell lines were treated for 24 h with 100 μmol/L Sal-B or 10 μmol/L celecoxib, alone and in half-dose of combination. The levels of cell viability were measured by MTT method compared with untreated cells. B, effect of Sal-B and celecoxib, alone and in combination, on cell cycle. JHU-022 cells were treated with Sal-B (100 μmol/L) and celecoxib (10 μmol/L), alone and in half-dose of combination. The cell cycle was analyzed by flow cytometry.

Table 1. Flow cytometric analysis of the effect of Sal-B (100 μmol/L) and celecoxib (10 μmol/L), alone or in combination (50 μmol/L Sal-B plus 5 μmol/L celecoxib), on JHU-022

JHU-022	24 h			48 h		
	G_0-G_1 (%)	S (%)	G_2-M (%)	G_0-G_1 (%)	S (%)	G_2-M (%)
Untreated	52.05	28.39	19.55	61.84	17.46	20.7
Sal-B	59.43	27.63	12.94	63.46	17.18	19.36
Celecoxib	62.81	24.05	13.14	68.98	11.62	19.4
Combination	67.81	18.17	14.02	72.95	6.77	20.28

the cell population. The G_0-G_1 phase was markedly higher in the combination treatment relative to either Sal-B or celecoxib treatment alone in 24 hours (68% combination versus ~59% Sal-B, 63% celecoxib) or the 48-hour treatment (73% combination versus ~63% Sal-B, 69% celecoxib). Interestingly, the combination treatment inhibited S phase significantly as well (Table 1).

Effect of Sal-B in combination with celecoxib on inhibition of JHU-013 tumor xenografts in athymic nude mice

The combination effect was further investigated in JHU-013 solid tumor xenografts in immunodeficient mice. The daily treatments were initiated a day after JHU-013 cells were transplanted into the nude mice. The doses for individual treatments were 40 mg/kg/d Sal-B and 2.5 mg/kg/d celecoxib. The single-agent treatments consisted of 80 mg/kg/d Sal-B or 5 mg/kg/d celecoxib administered via i.p. injection every day for 24 days. During this period, each mouse was manually examined for tumor volume at least four times. The combination treatment was most effective in suppressing tumor growth in athymic nude mice (Fig. 2A). Sal-B alone also resulted in significant inhibition of tumor growth. Animals treated with celecoxib alone generally did not show a reduction in tumor growth compared with the untreated group. It should be noted that one mouse in the celecoxib alone group died on experimental day 22. The average tumor weight in the combination group (0.100 ± 0.005 g) was significantly lower than the untreated control groups (0.208 ± 0.007 g), the Sal-B group (0.162 ± 0.010 g), and the celecoxib group (0.196 ± 0.213 g; $P < 0.01$; Fig. 2B).

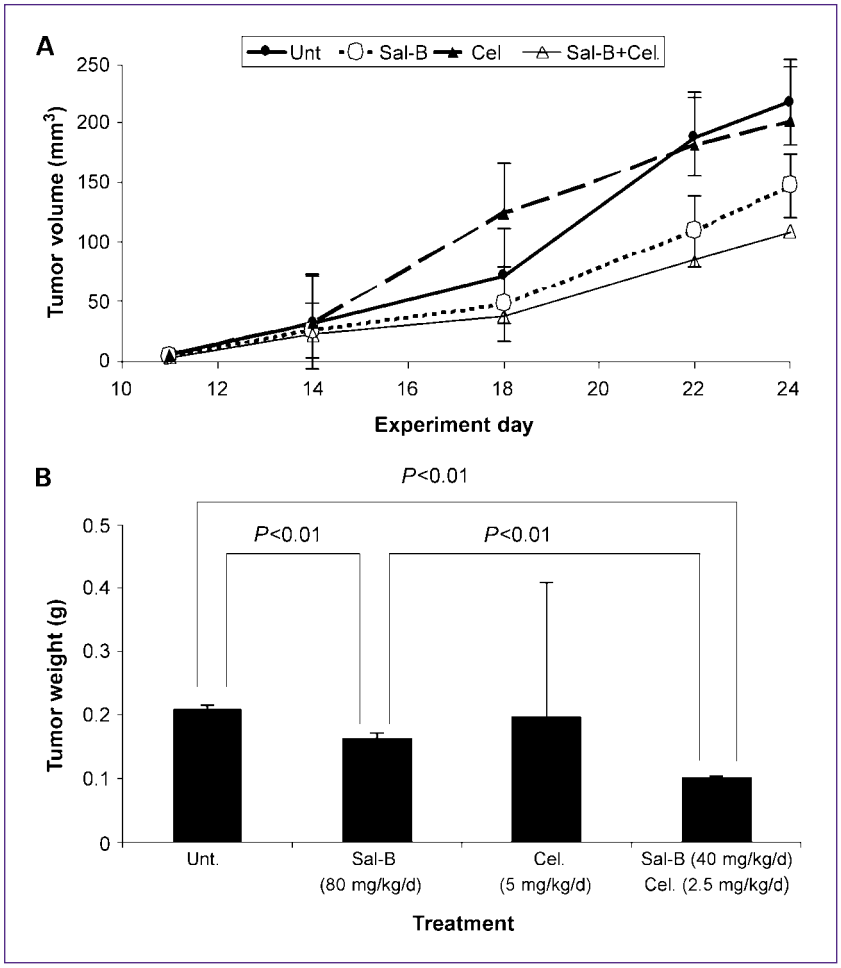

Fig. 2. Combination effect of Sal-B with celecoxib on inhibition of JHU-013 tumor xenografts in athymic nude mice. A, tumor growth curve, which was monitored periodically at different days during the 24-d experimental period. B, tumor weight, which was measured on the final experiment day. The *P* value was compared with untreated group.

Effect of Sal-B in combination with celecoxib on proliferation

Histologic sections were obtained from the JHU-013 xenografts and subsequently used to evaluate the single-agent and combination treatments on cell proliferation. A large necrotic area in the center of the tumor mass was present in all tumors from the control and single treatment groups, whereas the limited necrosis was found in combo treatment group that tumors were growing more slowly and did not outgrow their blood supply. The loose necrotic structure was visualized by H&E staining (Fig. 3A). PCNA, a proliferation biomarker, was analyzed by immunohistochemical staining (Fig. 3B). Statistics showed expression levels of PCNA that were significantly reduced in treated groups compared with untreated control ($P < 0.05$). However, there was no significant difference between the single and combination treatments (Fig. 3C).

Effect of Sal-B in combination with celecoxib on inhibition of COX-2 expression

The combination effect on the inhibition of COX-2 expression in HNSCC cell lines was also investigated *in vitro* and *in vivo*. COX-2 mRNA and protein levels were significantly reduced by either the single or the combination

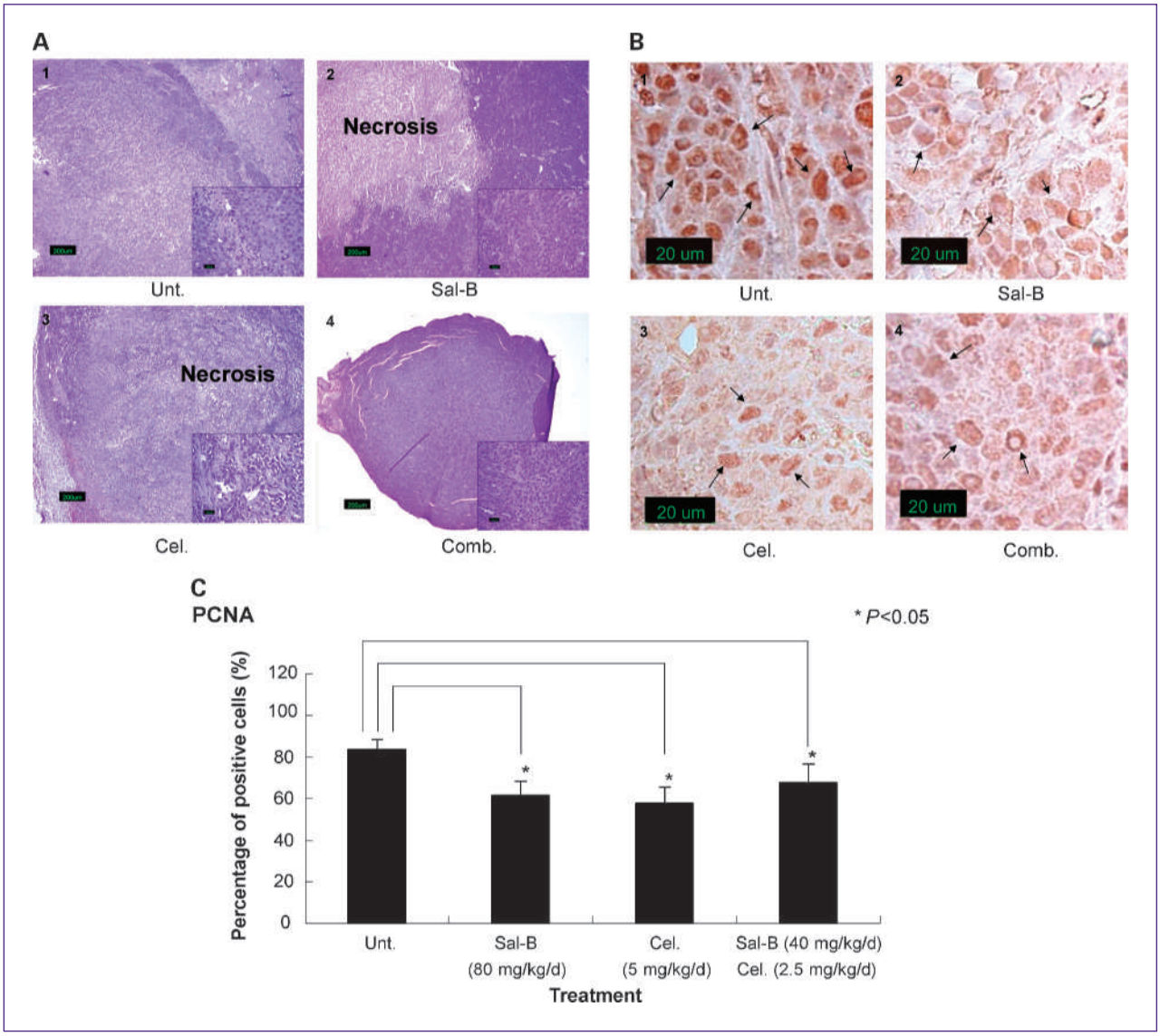

Fig. 3. Histopathology (H&E) images and immunohistochemical staining for PCNA in JHU-013 xenograft tumor masses of Sal-B and celecoxib, alone or in combination. A, H&E staining in tumor masses for each sample. 1, untreated group; 2, Sal-B treatment group; 3, celecoxib treatment group; 4, combination treatment group. Images were captured at ×40, and inset images (right bottom) were captured at ×400 magnification. B, expression of PCNA in different treatment groups in JHU-013 xenograft tissues. 1, untreated group; 2, Sal-B treatment group; 3, celecoxib treatment group; 4, combination treatment group. Scattered epithelial cell nuclei stained brown indicate PCNA expression. Images were captured at ×400 magnification. C, columns, mean PCNA expression levels in each group; bars, SE. *, $P < 0.05$.

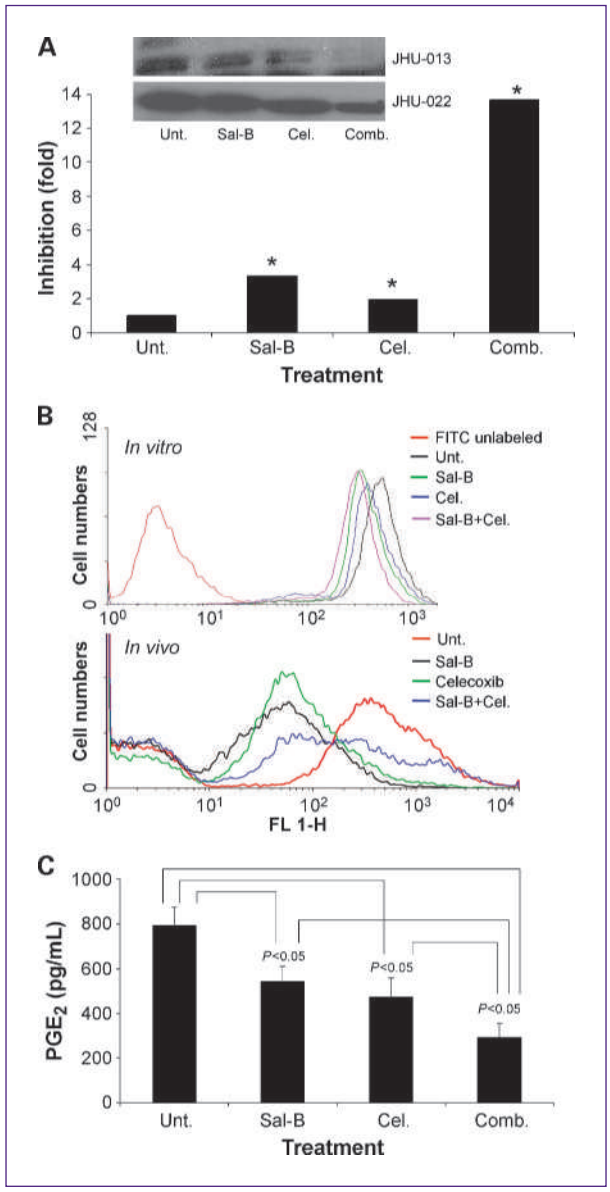

Fig. 4. Effect of Sal-B combined with celecoxib on inhibition of COX-2 expression. A, top, COX-2 protein, evaluated by Western blot after treatment of JHU-013 and JHU-022 cells with Sal-B and celecoxib, alone or in combination; bottom, COX-2 mRNA expression, measured by reverse transcription-PCR. B, COX-2 protein levels were analyzed by flow cytometry with FITC-conjugated COX-2 antibody after treatment of JHU-013 cells with Sal-B and celecoxib, alone or in combination. C, an enzyme immunoassay was used to determine the levels of PGE_2 in JHU-013 cells treated with Sal-B (100 μmol/L), celecoxib (10 μmol/L), and combination (50 μmol/L Sal-B plus 5 μmol/L celecoxib). *, $P < 0.05$, compared with untreated group.

treatment in JHU-013 and JHU-022. Western blot and quantitative real-time PCR analyses showed that the combined treatment was significantly more effective at inhibiting COX-2 expression than either single-agent treatment (Fig. 4A). There was an ~13-fold reduction of COX-2 mRNA as a result of combination treatment compared with untreated JHU-013 cells, whereas the levels of COX-2 mRNA were reduced only approximately 1- or 2-fold in the single treatment groups. Flow cytometry analysis illustrated that COX-2 protein levels were markedly reduced in the treated JHU-013 cells and in the cells obtained by disaggregation of JHU-013 solid tumor xenografts (Fig. 4B). The COX-2 protein levels in the isolated xenograft cells were significantly reduced in the treated groups. In contrast, the lowest COX-2 protein level was observed in the Sal-B–treated group. There was a broad peak of cell distribution in the combination group with a majority of low levels of COX-2 protein. There was 32% reduction in PGE_2 due to treatment with 100 μmol/L Sal-B alone and 40% reduction with 10 μmol/L celecoxib treatment compared with untreated JHU-013 cells (Fig. 4C). In addition, the PGE_2 level was significantly reduced by ~63% when JHU-013 cells were exposed to a combination of Sal-B (50 μmol/L) and celecoxib (5 μmol/L). The average level of PGE_2 was 292.7 pg/mL in combination treatment, 541.2 pg/mL in Sal-B treatment, and 471.4 pg/mL in celecoxib treatment, respectively.

Effect of Sal-B in combination with celecoxib on apoptosis

Cell apoptosis was determined by Western blot and TUNEL assay in the cultured HNSCC cells and JHU-013 xenografts. First, we measured the expression of the apoptosis-related proteins p53 and Bcl-2 after JHU-022 cells were exposed to Sal-B, celecoxib, and the combination (Fig. 5A). Our results showed that either the Sal-B single treatment or the combination resulted in an increased p53 protein level and decreased Bcl-2 level in JHU-022 cells. These results were not observed for celecoxib treatment alone. A significant change in the levels of proapoptotic p53 protein and antiapoptotic Bcl-2 protein was observed in the combination-treated cells. In addition, there was a significant reduction of EGFR protein level in the combination-treated cells. EGFR is one of the fundamental elements associated with COX-2 pathway contributing to the tumor growth and progression in many solid tumors. The apoptotic events were further detected by TUNEL assay in JHU-013 solid tumor xenografts (Fig. 5B). The low-dose combination treatment of Sal-B and celecoxib led to a higher number of apoptotic cells than the untreated or single treatment groups (Fig. 5C).

Discussion

HNSCC ranks among the six most common cancers in the world and is a significant cause of cancer morbidity and mortality (32). According to the American Cancer Society, ~35,000 new cases are diagnosed and 7,600 deaths occur annually in the United States. Despite advances in treatment, the overall 5-year survival rate has briefly improved in recent years, but the incidence of oral cavity and pharynx cancers continues to increase. In addition, African-American males have suffered the highest incidence of HNSCC and the lowest survival compared

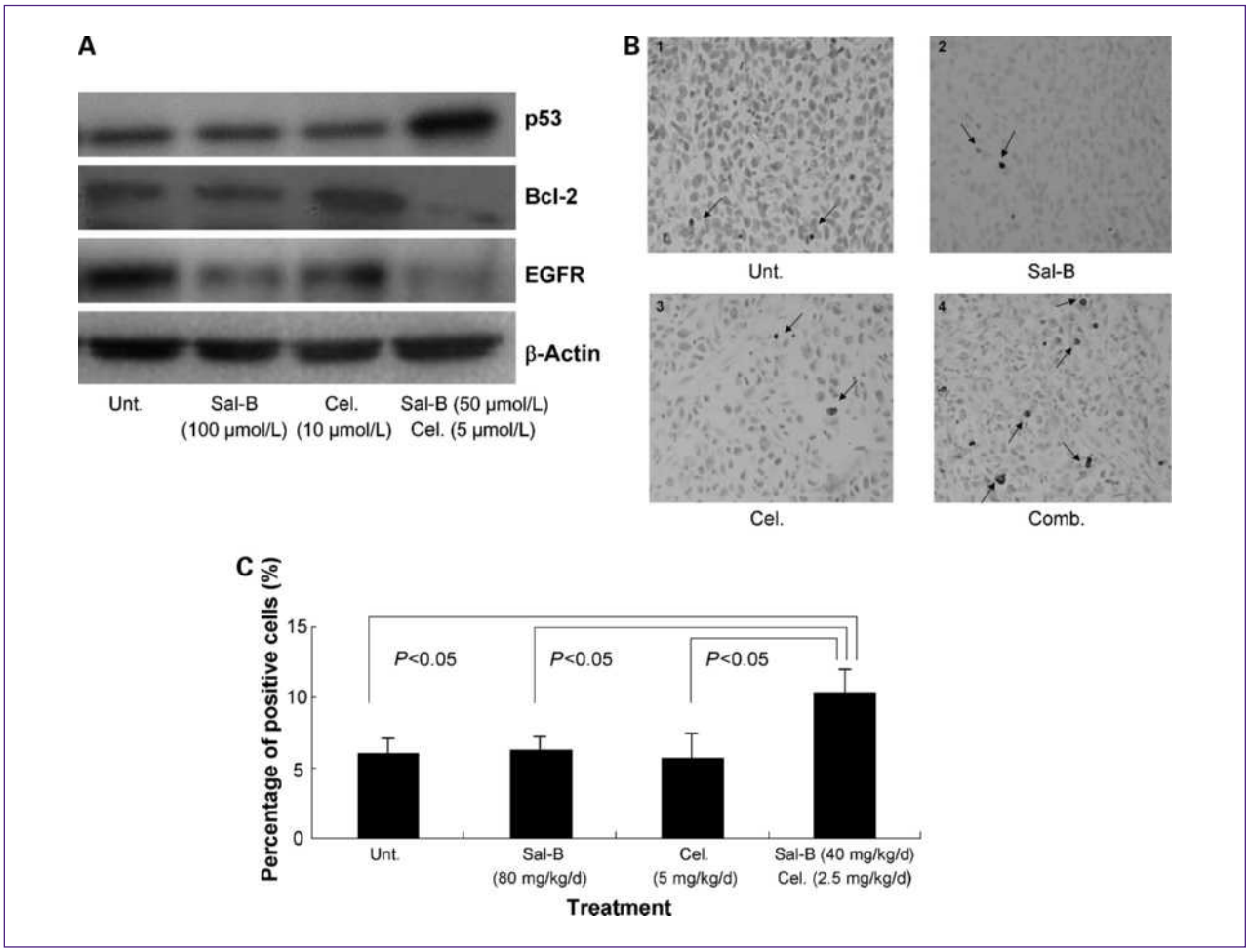

Fig. 5. Effect of Sal-B combined with celecoxib on induction of apoptosis *in vitro* and *in vivo*. A, *in vitro*, expression of apoptosis-related protein of p53, Bcl-2, and EGFR of JHU-022 exposed to Sal-B (100 μmol/L), celecoxib (10 μmol/L), and combination (50 μmol/L Sal-B and 5 μmol/L celecoxib) for 24 h. B, TUNEL staining in tumor masses. 1, untreated group; 2, Sal-B treatment group; 3, celecoxib treatment group; 4, combination treatment group. Nuclei were counterstained with methyl green (five mice per group). Images were captured at ×200 magnification. Arrows indicate apoptosis-positive cells. C, columns, mean apoptotic rate in each groups; bars, SE. $P < 0.05$.

with any racial/ethnic group (33). It urgently needs an effective, nontoxic, and affordable novel pharmacologic agent or drug to prevent development of HNSCC.

The idea that chronic inflammation shares pathways active in malignancy and can work in concert with genotoxic agents and participate in carcinogenesis is noted in many solid tumor systems. Therefore, blocking inflammation is thought to be a logical approach to cancer prevention therapy (34). COX-2, which has aberrant expression in many inflammation-associated tumors, is believed to be related to the development of cancer. Additionally, its principal metabolite PGE_2 seems to have pleiotropic effects on carcinogenesis, such as inducing tumor cell growth, inhibiting apoptosis, promoting tumor angiogenesis, and decreasing immunosurveillance (35). Therefore, COX-2 could be an ideal target for development of chemopreventive agents for cancer prevention; meanwhile, alterations to the COX-2/PGE_2 pathway are widely accepted, which have key roles in promoting tumor development.

Celecoxib is a selective COX-2 inhibitor, and its effectiveness for cancer prevention and therapy has been proven by a plethora of data, including colorectal cancer, prostate cancer, breast cancer, and HNSCC (36, 37). Although several tests of COX-2 inhibitors for cancer prevention were halted because of unacceptable cardiotoxicity, the debate on celecoxib reuse as a chemopreventive agent is appearing to intensify. Celecoxib has been shown to cause adverse cardiovascular effects when taken at high doses over a long duration (38). A report from a large-scale clinical trial indicated that the increased cardiovascular risk in celecoxib was only noted at daily doses of ≥400 mg (12, 37). In other words, the cardiovascular risk can be limited by reducing the dose of celecoxib, below 400 mg daily dose. In our study, with translation celecoxib dosage from human to mouse, the celecoxib dose in combination or single treatment is much lower than the suggested safe dose limit.

The combination of conventional cytotoxic drugs with other chemopreventive agents is an evolving trend in clinical practices for cancer treatment and prevention (39–41). Many studies reported that combination treatment not only could lead to increased anticancer efficacy but also reduced drug side effects. The strategy of this study is to apply a combination approach, Sal-B with low-dose celecoxib, to suppress HNSCC cell growth. There are three reasons why we were interested in the combination treatment: First, we found that Sal-B is capable of inhibiting tumor growth via blocking COX-2 expression and promoting apoptotic pathways (5); second, the combination with low dose of celecoxib may enhance the anti–COX-2 capacity in both COX-2 activity and expression; and third, the cardiovascular side effects of celecoxib may be also limited by reducing the dose of celecoxib and cardiovascular protection of Sal-B.

The outcomes showed that the combination treatment of Sal-B with low-dose celecoxib greatly enhanced the inhibition of HNSCC cell proliferation and cell viability compared with Sal-B or celecoxib alone in either cultured cells or tumor xenografts (Figs. 1 and 2). However, the response to the combination treatment varies in different HNSCC cell lines (Fig. 1A). It may depend on COX-2 expression level in the cell lines. For example, JHU-011, JHU-013, or JHU-022 cell lines have higher levels of COX-2 than JHU-06 (5). These three cell lines are more sensitive to the combination treatment than JHU-06. In addition, the combination treatment resulted in increased cell populations in G_1 phase and decreased populations in S phase in cell cycle experiment (Fig. 1B; Table 1). Cell proliferation was inhibited via DNA synthesis blockage. The results using tumor xenografts provided further support for the observations from cultured cells. The average tumor weight and volume in the combination group was significantly lower than that observed for the untreated and single-agent treatment groups. However, a large variation of tumor size was observed in the celecoxib alone–treated group (Fig. 2B). Although this phenomenon also occurred in our previous study, it remains to be determined if this death was due to celecoxib-related toxicity. Furthermore, a mouse in this group suffered dramatic body weight loss and died on day 22. These results indicate that the observed safety of celecoxib as used in this study is worthy of further investigation. *S. miltiorrhiza* Bge is regarded as a "panacea" for cardiovascular protection during its use over thousands of years in China due to its ability to promote blood circulation and remove blood stasis. Therefore, Sal-B, the major functional component of *S. miltiorrhiza* Bge, may be able to mediate the cardiovascular risk of celecoxib. The mechanism of celecoxib increasing cardiovascular risk is not clear, but there is some evidence that celecoxib might lower the production of prostacyclin without affecting the synthesis of thromboxane A_2, contributing to a prothrombotic state (42). Sal-B exerts cardiovascular prevention via making balance with prostacyclin and thromboxane A_2 (43). However, more studies are needed to provide further insight into this possibility.

Our previous study has shown that Sal-B effectively inhibits the levels of COX-2–related mRNA and protein in HNSCC (5). In this study, the enhanced effects of Sal-B and celecoxib on inhibition of COX-2 expression were clearly shown in *in vitro* tests, such as the levels of COX-2 mRNA and protein (Fig. 4A). In *in vivo* tests, the lowest COX-2 protein level was observed in the Sal-B–treated group analyzed by flow cytometry; however, a broad peak of low level of COX-2 protein was found in the combination-treated group (Fig. 4B). It is recognized that different tumor growth phases and the tumor microenvironment may cause a large range of COX-2 expression. Furthermore, COX-2 catalyzes the synthesis of prostaglandins, including PGE_2, from arachidonic acid. Overexpression of COX-2 in tumor cells is seen in conjunction with increased PGE_2 levels in HNSCC (44). PGE_2, as a principal metabolite of COX-2 pathway, affects multiple aspects of cell physiology involving cell survival, proliferation, migration, and invasion (45). The expression level of PGE_2 is significantly inhibited by the combination treatment (Fig. 4C). It has been reported that the COX-2/PGE_2 pathway likely plays a role along with other signaling pathways in regulating cancer development (34). Our studies show that the combination treatment exhibited enhanced inhibition of COX-2/PGE_2, induction of apoptosis, and regulation of EGFR expression (Fig. 5A).

In conclusion, Sal-B in combination with low-dose celecoxib can enhance the anticancer efficacy, particularly in chronic inflammatory-associated HNSCC, compared with high-dose Sal-B or celecoxib alone. The *in vitro* and *in vivo* lines of evidence show that the enhanced effects of the combination treatment on cell proliferation and cell death of HNSCC cells are through multiple pathways, such as sequential inhibition of the COX-2/PGE_2/EGFR pathway and induction of apoptosis. Additionally, the cardiotoxicity of celecoxib may be limited by lowering its dose. This combination strategy can be considered a new approach in targeting inflammatory-associated HNSCC prevention and treatment.

Disclosure of Potential Conflicts of Interest

No potential conflicts of interest were disclosed.

Acknowledgments

We thank Dan Zhang and Yongheng Dong for their excellent technical assistance and Liang Shan for valuable discussion.

Grant Support

NIH/National Cancer Institute grant CA118770, RCMI 2 G12 RR003048, and Tianjue Gu Foundation.

The costs of publication of this article were defrayed in part by the payment of page charges. This article must therefore be hereby marked *advertisement* in accordance with 18 U.S.C. Section 1734 solely to indicate this fact.

Received 11/16/2009; revised 01/08/2010; accepted 01/28/2010; published OnlineFirst 05/25/2010.

References

1. Pai SI, Westra WH. Molecular pathology of head and neck cancer: implications for diagnosis, prognosis, and treatment. Annu Rev Pathol 2009;4:49–70.
2. Mantovani A, Allavena P, Sica A, Balkwill F. Cancer-related inflammation. Nature 2008;454:436–44.
3. Kupferman ME, Myers JN. Molecular biology of oral cavity squamous cell carcinoma. Otolaryngol Clin North Am 2006;39:229–47.
4. Kelloff GJ, Lippman SM, Dannenberg AJ, et al. Progress in chemoprevention drug development: the promise of molecular biomarkers for prevention of intraepithelial neoplasia and cancer—a plan to move forward. Clin Cancer Res 2006;12:3661–97.
5. Hao Y, Xie T, Korotcov A, et al. Salvianolic acid B inhibits growth of head and neck squamous cell carcinoma *in vitro* and *in vivo* via cyclooxygenase-2 and apoptotic pathways. Int J Cancer 2009;124:2200–9.
6. Haddad RI, Shin DM. Recent advances in head and neck cancer. N Engl J Med 2008;359:1143–54.
7. Dajani EZ, Islam K. Cardiovascular and gastrointestinal toxicity of selective cyclo-oxygenase-2 inhibitors in man. J Physiol Pharmacol 2008;59 Suppl 2:117–33.
8. Schonthal AH, Chen TC, Hofman FM, Louie SG, Petasis NA. Celecoxib analogs that lack COX-2 inhibitory function: preclinical development of novel anticancer drugs. Expert Opin Investig Drugs 2008; 17:197–208.
9. Reddy BS, Patlolla JM, Simi B, Wang SH, Rao CV. Prevention of colon cancer by low doses of celecoxib, a cyclooxygenase inhibitor, administered in diet rich in ω-3 polyunsaturated fatty acids. Cancer Res 2005;65:8022–7.
10. Arber N, Eagle CJ, Spicak J, et al. Celecoxib for the prevention of colorectal adenomatous polyps. N Engl J Med 2006;355:885–95.
11. Lai V, George J, Richey L, et al. Results of a pilot study of the effects of celecoxib on cancer cachexia in patients with cancer of the head, neck, and gastrointestinal tract. Head Neck 2008;30:67–74.
12. Solomon SD, McMurray JJ, Pfeffer MA, et al. Cardiovascular risk associated with celecoxib in a clinical trial for colorectal adenoma prevention. N Engl J Med 2005;352:1071–80.
13. Bertagnolli MM, Eagle CJ, Zauber AG, et al. Five-year efficacy and safety analysis of the Adenoma Prevention with Celecoxib Trial. Cancer Prev Res (Phila Pa) 2009;2:310–21.
14. Huang WF, Hsiao FY, Wen YW, Tsai YW. Cardiovascular events associated with the use of four nonselective NSAIDs (etodolac, nabumetone, ibuprofen, or naproxen) versus a cyclooxygenase-2 inhibitor (celecoxib): a population-based analysis in Taiwanese adults. Clin Ther 2006;28:1827–36.
15. Wang X, Morris-Natschke SL, Lee KH. New developments in the chemistry and biology of the bioactive constituents of Tanshen. Med Res Rev 2007;27:133–48.
16. Lee AR, Wu WL, Chang WL, Lin HC, King ML. Isolation and bioactivity of new tanshinones. J Nat Prod 1987;50:157–60.
17. Liu J, Shen HM, Ong CN. *Salvia miltiorrhiza* inhibits cell growth and induces apoptosis in human hepatoma HepG(2) cells. Cancer Lett 2000;153:85–93.
18. Liu JJ, Zhang Y, Lin DJ, Xiao RZ. Tanshinone IIA inhibits leukemia THP-1 cell growth by induction of apoptosis. Oncol Rep 2009;21:1075–81.
19. Yin HQ, Choi YJ, Kim YC, Sohn DH, Ryu SY, Lee BH. *Salvia miltiorrhiza* Bunge and its active component cryptotanshinone protects primary cultured rat hepatocytes from acute ethanol-induced cytotoxicity and fatty infiltration. Food Chem Toxicol 2009;47:98–103.
20. Chen YL, Hu CS, Lin FY, et al. Salvianolic acid B attenuates cyclooxygenase-2 expression *in vitro* in LPS-treated human aortic smooth muscle cells and *in vivo* in the apolipoprotein-E-deficient mouse aorta. J Cell Biochem 2006;98:618–31.
21. Park JW, Lee SH, Yang MK, et al. 15,16-Dihydrotanshinone I, a major component from *Salvia miltiorrhiza* Bunge (Dansham), inhibits rabbit platelet aggregation by suppressing intracellular calcium mobilization. Arch Pharm Res 2008;31:47–53.
22. Liu CSCY, Hu JF, Zhang W, Chen NH, Zhang JT. Comparison of antioxidant activities between salvianolic acid B and *Ginkgo biloba* extract (EGb 761). Acta Pharmacol Sin 2006;27:1137–45.
23. Tsai MK, Lin YL, Huang YT. Effects of salvianolic acids on oxidative stress and hepatic fibrosis in rats. Toxicol Appl Pharmacol 2010;242:155–64.
24. Zhou ZT, Yang Y, Ge JP. The preventive effect of salvianolic acid B on malignant transformation of DMBA-induced oral premalignant lesion in hamsters. Carcinogenesis 2006;27:826–32.
25. Bi XB, Deng YB, Gan DH, Wang YZ. Salvianolic acid B promotes survival of transplanted mesenchymal stem cells in spinal cord-injured rats. Acta Pharmacol Sin 2008;29:169–76.
26. Liu CL, Xie LX, Li M, Durairajan SS, Goto S, Huang JD. Salvianolic acid B inhibits hydrogen peroxide-induced endothelial cell apoptosis through regulating PI3K/Akt signaling. PLoS One 2007;2:e1321.
27. Falandry C, Canney PA, Freyer G, Dirix LY. Role of combination therapy with aromatase and cyclooxygenase-2 inhibitors in patients with metastatic breast cancer. Ann Oncol 2009;20:615–20.
28. Reddy BS. Strategies for colon cancer prevention: combination of chemopreventive agents. Subcell Biochem 2007;42:213–25.
29. Hamakawa H, Nakashiro K, Sumida T, et al. Basic evidence of molecular targeted therapy for oral cancer and salivary gland cancer. Head Neck 2008;30:800–9.
30. Gupta RA, DuBois RN. Combinations for cancer prevention. Nat Med 2000;6:974–5.
31. Livak KJST. Analysis of relative gene expression data using real-time quantitative PCR and the $2(-\Delta\Delta C(T))$ method. Methods 2001; 25:402–8.
32. Parkin DM. Global cancer statistics in the year 2000. Lancet Oncol 2001;2:533–43.
33. Carroll WR, Kohler CL, Carter VL, Hannon L, Skipper JB, Rosenthal EL. Barriers to early detection and treatment of head and neck squamous cell carcinoma in African American men. Head Neck 2009;31:1557–62.
34. Anderson WF, Umar A, Hawk ET. Cyclooxygenase inhibition in cancer prevention and treatment. Expert Opin Pharmacother 2003; 4:2193–204.
35. Greenhough A, Smartt HJ, Moore AE, et al. The COX-2/PGE2 pathway: key roles in the hallmarks of cancer and adaptation to the tumour microenvironment. Carcinogenesis 2009;30:377–86.
36. Subbaramaiah K, Dannenberg AJ. Cyclooxygenase 2: a molecular target for cancer prevention and treatment. Trends Pharmacol Sci 2003;24:96–102.
37. Bonovas S, Tsantes A, Drosos T, Sitaras NM. Cancer chemoprevention: a summary of the current evidence. Anticancer Res 2008;28:1857–66.
38. Fitzgerald GA. Coxibs and cardiovascular disease. N Engl J Med 2004;351:1709–11.
39. Ignatenko NA, Besselsen DG, Stringer DE, Blohm-Mangone KA, Cui H, Gerner EW. Combination chemoprevention of intestinal carcinogenesis in a murine model of familial adenomatous polyposis. Nutr Cancer 2008;60 Suppl 1:30–5.
40. Meyskens FL, Jr., McLaren CE, Pelot D, et al. Difluoromethylornithine plus sulindac for the prevention of sporadic colorectal adenomas: a randomized placebo-controlled, double-blind trial. Cancer Prev Res (Phila Pa) 2008;1:32–8.
41. Xiao H, Yang CS. Combination regimen with statins and NSAIDs: a promising strategy for cancer chemoprevention. Int J Cancer 2008; 123:983–90.
42. Yamamoto T, Kakar NR, Vina ER, Johnson PE, Bing RJ. Effect of cyclooxygenase-2 inhibitor (celecoxib) on the infarcted heart *in situ*. Pharmacology 2001;63:28–33.
43. Adams JD, Wang R, Yang J, Lien EJ. Preclinical and clinical examinations of *Salvia miltiorrhiza* and its tanshinones in ischemic conditions. Chin Med 2006;1:3.
44. Camacho M, Leon X, Fernandez-Figueras MT, Quer M, Vila L. Prostaglandin E(2) pathway in head and neck squamous cell carcinoma. Head Neck 2008;30:1175–81.
45. Wang F, Arun P, Friedman J, Chen Z, Van Waes C. Current and potential inflammation targeted therapies in head and neck cancer. Curr Opin Pharmacol 2009;9:389–95.